scientific reports

Check for updates

OPEN

Bifidobacterium breve promotes growth and lipid alteration in *Trichomonas vaginalis* transiently through transcriptomic reprogramming

Pei-Yun Chen[1,9], Yuan-Ming Yeh[2,3,4,9], Chun-Hsien Chen[4,5], Ming-Chi Li[6,7], Yu-Tzu Hsu[7], Po-Jung Huang[2,8]✉ & Wei-Hung Cheng[1]✉

Trichomonas vaginalis **is recognized as the most prevalent non-viral sexually transmitted parasitic infection, establishing its presence in the vaginal microbiota alongside commensal bacteria, particularly** ***Lactobacillus*** **and** ***Bifidobacterium*** **species. Notably, a reduction in the population of** ***Bifidobacterium breve*** **has been documented in women infected with** ***T. vaginalis***. **However, the dynamics of the interaction between** ***T. vaginalis*** **and these beneficial bacterial species remain inadequately understood, warranting further investigation to elucidate the underlying mechanisms and potential implications for vaginal health. We investigated the effects of** ***B. breve*** **on the growth of** ***T. vaginalis*****, including its gene expression and interactions with the host. HeLa cells were exposed to** ***T. vaginalis*** **that had been pretreated with or without** ***B. breve***. **We assessed cytokine responses (specifically IL-6 and IL-8) and evaluated cytopathic effects. The dynamics of the co-culture were monitored microscopically. Additionally, we conducted transcriptomic and metabolomic analyses to characterize the responses of** ***T. vaginalis*** **to** ***B. breve***. **Co-culture of** ***T. vaginalis*** **with** ***B. breve*** **for 4 h significantly increased protozoan proliferation by 1.2-fold, while bacterial abundance was reduced by 27%. HeLa cells showed no cytopathic effects or changes after treatment with** ***B. breve*****, whether given before or alongside** ***T. vaginalis***. **Microscopy showed a direct physical association between the two organisms. Transcriptomic profiling of** ***T. vaginalis*** **co-cultured with** ***B. breve*** **revealed an upregulation of genes related to fatty acid metabolism and DNA replication. Metabolomic analysis confirmed changes in the content of long-chain fatty acids. Additionally, there was an increase in virulence-associated genes, including adhesins.** ***B. breve*** **promotes the growth of** ***T. vaginalis*** **and modulates parasite gene expression and lipid metabolism transiently. However, it does not confer protection on host epithelial cells during infection. These findings suggest that** ***B. breve*** **may contribute to maintaining microbial community balance but does not directly counteract** ***T. vaginalis***. **Importantly, these insights highlight the potential value of** ***B. breve*****–associated microbial or metabolic signatures as indicators of ecological shifts that predispose to parasite overgrowth.**

Keywords *Bifidobacterium breve*, Protozoan-prokaryote interaction, Fatty acid metabolism, Transcriptomics, *Trichomonas vaginalis*

[1]Department of Parasitology, College of Medicine, National Cheng Kung University, Tainan, Taiwan. [2]Genomic Medicine Core Laboratory, Chang Gung Memorial Hospital, Linkou, Taiwan. [3]Graduate Institute of Health Industry Technology, Chang Gung University of Science and Technology, Taoyuan, Taiwan. [4]Graduate Institute of Biomedical Sciences, College of Medicine, Chang Gung University, Taoyuan, Taiwan. [5]Department of Parasitology, College of Medicine, Guishan Dist., Chang Gung University, Taoyuan City, Taiwan. [6]Division of Infectious Diseases, Department of Internal Medicine, College of Medicine, National Cheng Kung University Hospital, National Cheng Kung University, Tainan, Taiwan. [7]Department of Medicine, College of Medicine, National Cheng Kung University, Tainan, Taiwan. [8]Department of Biomedical Sciences, College of Medicine, Guishan Dist., Chang Gung University, Taoyuan City, Taiwan. [9]Pei-Yun Chen and Yuan-Ming Yeh contributed equally to this work. ✉email: pjhuang@gap.cgu.edu.tw; whcheng@gs.ncku.edu.tw

Abbreviations

IL	Interleukin
HIV	Human immunodeficiency virus
HPV	Human papillomavirus
PFOR	Pyruvate ferredoxin oxidoreductase
APs	Adhesion proteins
PCR	Polymerase chain reaction
BV	Bacterial vaginosis
CST	Community-state type
EV	Extracellular vesicle
FAS	Fatty acid synthesis
DAPI	4',6-diamidino-2-phenylindole
CFU	Colony-forming unit
PCA	Principal component analysis
GSEA	Gene set enrichment analysis
GO	Gene ontology
KEGG	Kyoto Encyclopedia of Genes and Genomes
GSVA	Gene set variation analysis
SCFA	Short-chain fatty acid
SFA	Saturated fatty acids
UFA	Unsaturated fatty acids

Trichomonas vaginalis is a flagellated protozoan that infects the human urogenital tract, leading to trichomoniasis, the most common non-viral sexually transmitted infection worldwide. According to the World Health Organization, approximately 276 million new cases are diagnosed each year[1]. Infected women often experience symptoms such as vaginal discharge, pain, and inflammation. In contrast, most infected men remain asymptomatic, with only a small percentage developing urethritis or prostatitis[1]. In addition to its clinical symptoms, infection with *T. vaginalis* is linked to an increased risk of acquiring human immunodeficiency virus (HIV), persistence of human papillomavirus (HPV), and the development of cervical cancer[2]. Although trichomoniasis is not directly fatal, its significance in epidemiology highlights the necessity for ongoing research.

The vaginal microbiota forms a key defense against pathogens by maintaining mucosal homeostasis and preventing colonization through mechanisms such as competitive exclusion and immune modulation[3]. The vaginal community has been classified into five community-state types (CSTs). CST I, II, and V, dominated by *Lactobacillus crispatus*, *L. gasseri*, and *L. jensenii*, are protective, whereas CST III and CST IV, characterized by *L. iners* and diverse anaerobes, respectively, are linked to dysbiosis and infection[4,5]. In healthy women, *Bifidobacterium breve* is also abundant, particularly in CST I and II[6,7].

B. breve is a Gram-positive anaerobe commonly found in the gut, vagina, and oral cavity[8]. As a probiotic commensal bacterium, it promotes epithelial barrier integrity, modulates immune responses, and produces lactic acid, which helps maintain acidic vaginal pH and suppresses pathogen overgrowth[9–11]. Lactic acid not only inhibits bacteria associated with bacterial vaginosis but also regulates epithelial function and reduces susceptibility to infections such as *Chlamydia trachomatis*. Notably, the abundance of *B. breve* significantly decreases during *T. vaginalis* infection[12]. This reduction suggests a disruption of normally protective microbial members during parasite overgrowth. However, despite its well-established beneficial roles in vaginal homeostasis, the influence of *B. breve* on *T. vaginalis* biology and the mechanisms underlying their interaction remain unclear. This knowledge gap highlights the importance of characterizing how *B. breve* affects parasite physiology and its potential contribution to microbial community shifts during infection.

The interplay between vaginal microbes and *T. vaginalis* can profoundly affect infection outcomes. *Lactobacillus gasseri* reduces host cell damage by decreasing the adhesion of *T. vaginalis* onto host epithelium, and the secreted products exhibit parasiticidal activity against trichomonad infection[13,14]. Similarly, bacterial extracellular vesicles (EVs), which carry proteins, nucleic acids, lipids, and metabolites[15], modulate parasite adhesion and host cell interaction. EVs from commensal bacteria promote host defense[16,17], whereas those from BV-associated bacteria, such as *G. vaginalis*, enhance parasite internalization[15]. Furthermore, both CST-IV bacteria and *T. vaginalis* compromise tight junction integrity, increasing paracellular permeability, and disrupting the epithelial barrier[18–23].

In addition to microbial interactions, lipid metabolism is vital for protozoan survival and virulence. Fatty acids are essential structural components of membranes, energy sources, and signaling molecules[24]. Fatty acid synthesis (FAS) pathways vary among protozoa, with some species utilizing FAS-I or FAS-II systems[25–27]. Fatty acids also participate in host-pathogen interactions; for instance, *Trypanosoma cruzi* manipulates host lipid signaling to facilitate invasion[28,29]. Unlike other protozoa, *T. vaginalis* lacks a de novo FAS pathway and depends on exogenous fatty acids, linking its pathogenicity to host lipid availability[30]. Given that commensal bacteria can influence local lipid availability and metabolism, they may indirectly shape *T. vaginalis* physiology.

In light of the essential roles of vaginal microbial communities and parasite lipid metabolism in shaping *T. vaginalis* infection dynamics, elucidating how *B. breve* influences parasite behavior is of particular importance. This study therefore investigates the interactions between *B. breve* and *T. vaginalis*, examines the resulting effects on parasite growth and physiology, and assesses the consequences for host–parasite interactions. By characterizing these microbe–parasite dynamics, our work provides new insights into the ecological and metabolic factors that may contribute to parasite overgrowth and may inform the development of microbiome-informed strategies for managing trichomoniasis.

Methods

Parasite and bacterial cultures

T. vaginalis (ATCC 30236) was cultured in YI-S medium[30], and serum-free YI-S (horse serum replaced by ddH_2O) was used for experimental treatments. The medium contained a vitamin mixture (#18), which was sterile-filtered prior to use. *B. breve* (ATCC 15700) was maintained anaerobically in Bifidobacterium broth, streaked to isolate single colonies, and preserved at −80°C in 50% glycerol. These cultures served as the basis for parasite-bacterium interaction studies.

Co-culture assay and *B. breve* pre-treated *T. vaginalis*

Co-culture experiments were conducted to investigate the direct interactions between *T. vaginalis* and *B. breve*. Mid-log phase bacteria and parasites were adjusted to 10^8 CFU and 10^7 cells, respectively. The ratio used in the co-culture assay followed that of the previous study[12]. Both organisms were combined in serum-free YI-S and incubated anaerobically for four hours. Cell viability and bacterial counts were monitored at sequential time points to assess the mutual growth dynamics. Each experiment was performed with three biological replicates. After the same treatment, *T. vaginalis* cells (1.5×10^5 cells) were subsequently used for co-culture with HeLa cells (2.5×10^6 cells) (Figure 3).

Tri-culture assay (pre-treatment): prior colonization by *B. breve*

HeLa cells were purchased from ATCC, The culture medium is Dulbecco's Modified Eagle Medium (DMEM; Gibco, Thermo Fisher Scientific, Cat# 12100046) with 10 % fetal bovine serum and 1 % antibiotic (GeneDireX, Cat# CC502-0100) were used as a host model to evaluate the effects of the microbes on epithelial cells. HeLa cells (2.5×10^6 cells/mL) were seeded in 24-well plates and incubated for 24 h before treatment. For the pretreated *B. breve* experiments, cells were pretreated with 5×10^7 CFU *B. breve* (live or heat-killed) followed by the addition of 2.5×10^6 *T. vaginalis* cells in a total volume of 1 mL serum-free DMEM. To establish comparative conditions, *T. vaginalis* or *B. breve* was cultured alone under the same conditions. Untreated HeLa cells cultured in serum-free DMEM served as the negative control. The tri-cultures were incubated for 6 or 12 hours to compare host responses under different conditions. Each experiment was performed with three biological replicates.

Tri-culture assay (co-treatment): simultaneous competition

For the simultaneous competition experiments, HeLa cells were co-treated with 5×10^7 CFU *B. breve* (live or heat-killed) and 2.5×10^6 *T. vaginalis* cells in a total volume of 1 mL serum-free DMEM. To establish comparative conditions, *T. vaginalis* or *B. breve* was cultured alone under the same conditions. Untreated HeLa cells cultured in serum-free DMEM served as the negative control. The tri-cultures were incubated for 6 or 12 hours to compare host responses under different conditions. Each experiment was performed with three biological replicates.

Microscopy and staining

Confocal microscopy was used to assess morphological alterations and microbial interactions. After co-culture with *B. breve*, *T. vaginalis* samples and *T. vaginalis* which cultured in serum-free YI-S served as the negative control were stained with 4',6-diamidino-2-phenylindole (DAPI) and visualized using confocal microscopy with a 100× oil immersion and a 405 nm laser. Choose an image size of 1,024 × 1,024 pixels and a scanning speed of 8.0 µs/ pixel to obtain high-quality images.

HeLa cells were treated according to the previously described procedure, followed by Giemsa staining for tri-culture assays to evaluate structural changes. The supernatants were collected for downstream cytokine analysis. HeLa cells were washed three times with phosphate-buffered saline (PBS) and fixed with a fixation solution for 30 minutes at room temperature, followed by overnight incubation with Giemsa solution. Images were quantitatively analyzed using CellProfiler, which measured the host cell area while excluding parasite interference. This analysis provided insights into the effects of microbes on host cell morphology.

RNA sequencing and analysis

T. vaginalis co-cultured with *B. breve* for 4 hours was collected with pre-warmed PBS washing steps, and *T. vaginalis* alone (negative control) was transferred into centrifuge tubes and centrifuged at a low speed (2,500 rpm for 5 minutes) to minimize bacterial cells co-pelleting. The supernatant was removed, and TRIzol reagent was added and mixed thoroughly. Total RNA was purified (Zymo Research, #R2052), and poly(A)-tailed mRNA was enriched using the Illumina Poly(A) Selection Kit (#20777928). The purified mRNA was fragmented and converted into double-stranded cDNA using the Illumina cDNA Synthesis Module (#20761354), followed by library construction (end repair, A-tailing, adaptor ligation, and PCR enrichment) with the Illumina RNA Prep, Ligation kit (#20778789). The library was constructed using Illumina Transcriptomic profiling of *T. vaginalis* was performed to identify the changes in gene expression induced by the experimental treatments. Total RNA was sequenced on the Illumina NovaSeq platform. Each experiment was performed with three biological replicates. Processed reads were mapped to the *T. vaginalis* G3 reference genome (TrichDB-65), and differential gene expression was analyzed using the DESeq2 package. Enrichment analyses, including ORA, GSEA, and GSVA, were performed using R to determine the affected biological pathways. Pathway maps were generated using KEGG (Kyoto Encyclopedia of Genes and Genomes)[31].

Metabolomics analysis

Metabolomic analyses were conducted to characterize the lipid alterations in parasite-bacterium interactions. After co-culture, the culture medium was transferred to centrifuge tubes and centrifuged at 2,500 rpm for 5 min. The resulting pellets were resuspended in 1 mL of 80% methanol and stored at −80 °C until analysis. For lipid

extraction, 300 µL of the methanolic cell suspension was mixed with 30 µL of methanol, followed by the addition of 900 µL of methyl tert-butyl ether (MTBE) containing an internal standard (Avanti Polar Lipids, Alabaster, AL, USA). The mixture was vortexed for over 1 min and incubated at room temperature for 60 min. Subsequently, 156 µL of water was added, and the sample was centrifuged at 12,000 ×g for 30 min at 4 °C. The upper organic phase was collected and evaporated to dryness under a gentle nitrogen stream. After KOH-mediated lipid hydrolysis, the dried residue was reconstituted in 200 µL of isopropanol/acetonitrile/water (2:1:1, v/v/v) and centrifuged again at 12,000 ×g for 30 min at 4 °C. The resulting supernatant was used for fatty acid analysis by ultra-high-performance liquid chromatography (UHPLC) coupled with a Xevo TQ-S triple quadrupole mass spectrometer (Waters Corp., Milford, MA, USA). Protein-normalized data were used to quantify the fatty acid profiles, providing insights into the lipid metabolic reprogramming associated with microbial interactions. Chromatographic separation was performed on a Waters ACQUITY CORTECS C18 column (2.1 mm × 150 mm, 1.6 µm) maintained at 60 °C. The mobile phases consisted of solvent A (acetonitrile/water, 20:80, v/v, with 0.01% formic acid) and solvent B (isopropanol/acetonitrile, 50:50, v/v, with 0.01% formic acid). The flow rate was 0.50 mL/min. The elution gradient started at 50% B, increased linearly to 70% B over 4 min, then to 98% B at 6.1 min, and was maintained for 1.3 min before returning to initial conditions and equilibrating for over 2 min. Mass spectrometric detection was performed in negative electrospray ionization (ESI) mode with a capillary voltage of 2000 V and a sampling cone voltage of 45 V. The desolvation gas flow was 1000 L/h, cone gas flow 150 L/h, desolvation temperature 500 °C, and source temperature 150 °C. Quality control (QC) samples and pooled QC samples (prepared by mixing aliquots of all samples) were analyzed throughout the run, with one QC injection after every 10 samples. Protein concentrations in the analyzed samples were determined using the Bradford assay and used to normalize the lipid extraction data. Each experiment was performed with four biological replicates.

Image analysis

Quantitative analysis of HeLa cell morphology was performed using the CellProfiler software. Images from Giemsa-stained cells were segmented using adaptive thresholding to accurately measure the cell area, while non-cellular elements and parasites were excluded. This approach allows for an objective assessment of host cell structural changes.

Cytokine measurement

The concentrations of IL-6 and IL-8 in culture supernatants were quantified using sandwich ELISA using an IL-6 ELISA assay (#430501; BioLegend, San Diego, CA, USA) and IL-8 ELISA assay (#431501; BioLegend, San Diego, CA, USA)as described previously[32,33]. Tri-culture supernatants were collected and centrifuged at 1,500 rpm to remove dead cells and debris. This assay detects cytokines through specific antibody binding and enzymatic color development, with the sample concentrations calculated from standard curves. Read the absorbance at 450 nm and 570 nm. The absorbance at 570 nm can be subtracted from that at 450 nm to correct for optical imperfections or background. These measurements provide a sensitive evaluation of inflammatory responses under various experimental conditions. Final cytokine levels are displayed as fold change of the control in the figures. Each experiment was performed with three biological replicates.

Statistical analysis

The Student's t-test was used to quantify the experimental results using GraphPad Prism 10. Asterisks represent the significance of each assay as determined by the *P*-value (* $p < 0.05$; ** $p < 0.01$; *** $p < 0.001$).

Results

B. breve enhanced the growth of *T. vaginalis*

B. breve is considered the second most abundant beneficial commensal species in the human vaginal microbiota, and a marked reduction in its abundance has been reported in STD patients co-infected with *T. vaginalis*[6,12]. However, its role during *T. vaginalis* infection remains underexplored. To investigate potential interactions between the two organisms, *T. vaginalis* and *B. breve* were co-cultured at a 1:10 ratio under anaerobic conditions for 4 h, as previously described[12,34]. Viable *T. vaginalis* counts and *B. breve* colony-forming units (CFUs) were assessed at 0, 1, 2, and 4 hours.

Parasite viability did not differ significantly from the control during the first 2 hours (Fig. 1A). By 4 hours, *T. vaginalis* showed a significant increase in viable counts compared with the untreated control (Fig. 1B). In contrast, *B. breve* CFUs declined significantly by the 2-hour time point and continued to decrease thereafter (Fig. 1B). These observations indicated that *B. breve* enhances the short-term growth of *T. vaginalis*, while its own viability was adversely affected during co-culture. Based on the enhanced protozoan viability observed at 4 hours, this condition was selected for subsequent experiments.

Direct interaction between *T. vaginalis* and *B. breve* during co-culture

To visualize the interaction between *T. vaginalis* and *B. breve*, confocal microscopy was performed following a 4-hour co-culture, the time point at which a significant increase in trichomonad viability was observed. *T. vaginalis* cells were stained with DAPI, fixed, and mounted for imaging. Representative confocal images are presented in Fig. 2A–F, with continuous video recordings available in **Movie S1**. In the co-culture group, *B. breve* cells were found closely surrounding the surface of *T. vaginalis* (Fig. 2D–F), suggesting a direct physical association between the two organisms under the in vitro culture conditions examined.

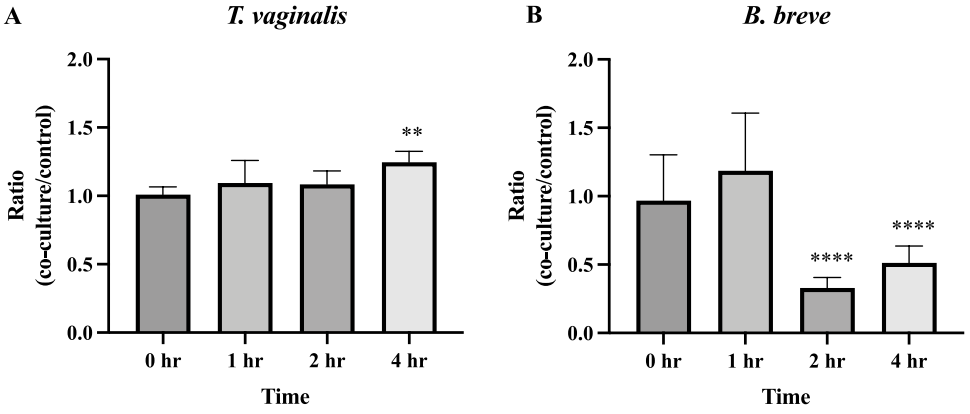

Fig. 1. Growth of *T. vaginalis* and reduction in *B. breve* colony-forming units (CFU) during co-culture. *T. vaginalis* and *B. breve* were co-cultured in serum-free YI-S medium at an initial ratio of 1:10. Monocultures of each organism served as controls. The X-axis indicates co-culture duration, and the Y-axis shows the relative counts or CFU of *T. vaginalis* (**A**) and *B. breve* (**B**) compared with their respective controls. Statistical significance: **p* < 0.05; ****p** < 0.01; *****p** < 0.001; ******p** < 0.0001.

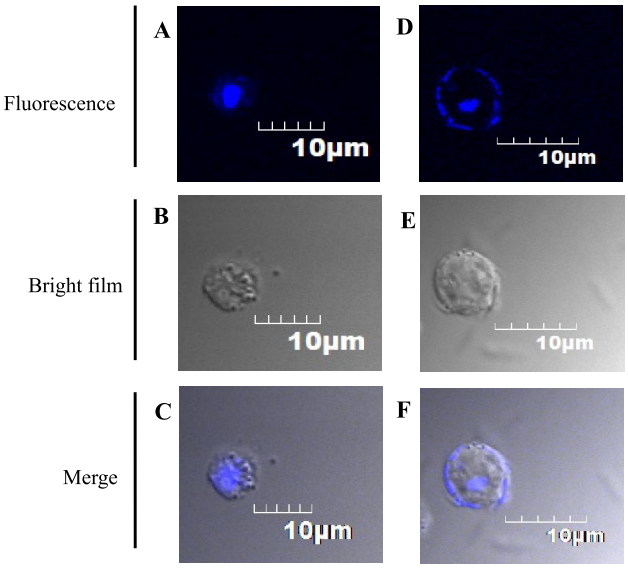

Fig. 2. Localization of *B. breve* on the surface of *T. vaginalis* during co-culture. *T. vaginalis* and *B. breve* were co-cultured for 4 hours and stained with DAPI for confocal microscopy. Panels (**A–C**): *T. vaginalis* monoculture. Panels (**D–F**): Co-culture of *T. vaginalis* and *B. breve*.

B. breve pre-colonization does not confer cytoprotection against *T. vaginalis* infection

Previous studies have suggested that vaginal commensal bacteria may exert cytoprotective effects or contribute to maintaining microbiota stability during *T. vaginalis* infection[14,35]. To clarify the role of *B. breve* in this context, we first evaluated whether pre-exposure of *T. vaginalis* to *B. breve* modulates the inflammatory response in HeLa cells. HeLa cells were incubated for 24 h with *T. vaginalis* that had been pretreated with or without *B. breve* for 4 hours, and IL-6 secretion was quantified. As shown in Fig. 3A, T. *vaginalis* infection increased in IL-6 secretion approximately two-fold relative to uninfected controls. Notably, IL-6 levels were further elevated in cells infected with *B. breve*-pretreated *T. vaginalis*, suggesting that *B. breve* did not attenuate the inflammatory response and may even enhance it.

Next, we investigated whether *B. breve* exerts a cytoprotective effect when pre-colonizing host epithelial cells. HeLa cells were pretreated with viable bacteria prior to *T. vaginalis* infection, with heat-killed *B. breve* used as an inactivated control. No significant difference in cell confluence (Fig. 3B–E) was observed between infected and uninfected cells pretreated with viable *B. breve*. Similarly, projected cell area measurements indicated that pretreatment with heat-killed *B. breve* did not alter the cell morphology induced by *T. vaginalis* (Fig. 3B and D).

To further assess inflammatory responses, IL-6 and IL-8 levels were measured at 6 and 12 h post-infection. As expected, IL-6 levels did not differ significantly between infected and uninfected cells, regardless of *B. breve* pretreatment (Fig. 4). In contrast, IL-8 levels were transiently elevated at the 6-hour time point in HeLa cells

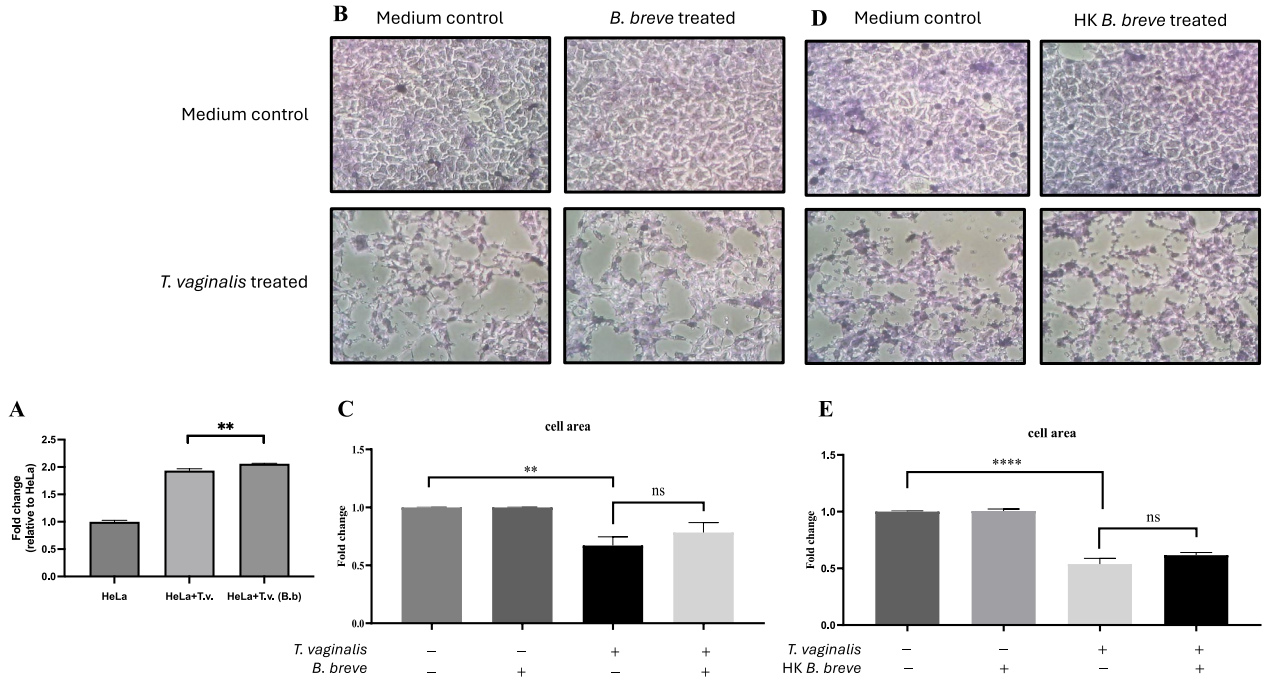

Fig. 3. *B. breve* does not exhibit cytoprotective activity during *T. vaginalis* infection. (**A**) The secretions of IL-6 from HeLa cells infected with *T. vaginalis* and *B. breve*-treated *T. vaginalis* were determined after 24 hours of incubation. The treated cells were washed, incubated, stained with Giemsa, and monitored under a microscope: (**B**) upper left, HeLa cells only; upper right HeLa cells treated with *B. breve* for 3 hours and cultured in serum- and antibiotic-free DMEM for 12 hours; lower left, HeLa cells were co-cultured with *T. vaginalis* in serum- and antibiotic-free DMEM for 12 hours; lower right, HeLa cells were pretreated with *B. breve* in serum- and antibiotic-free DMEM for 3 hours, followed by infection with *T. vaginalis* under the same conditions for 12 hours. (**C**) The quantified chart of (B). (**D**) The same settings as B were applied for heat-killed *B. breve* (HK-Bb) instead of viable *B. breve*. (**E**) The quantified chart of (D). Statistical significance: $^{*}p < 0.05$; $^{**}\mathbf{p} < 0.01$; $^{***}\mathbf{p} < 0.001$; $^{****}\mathbf{p} < 0.0001$.

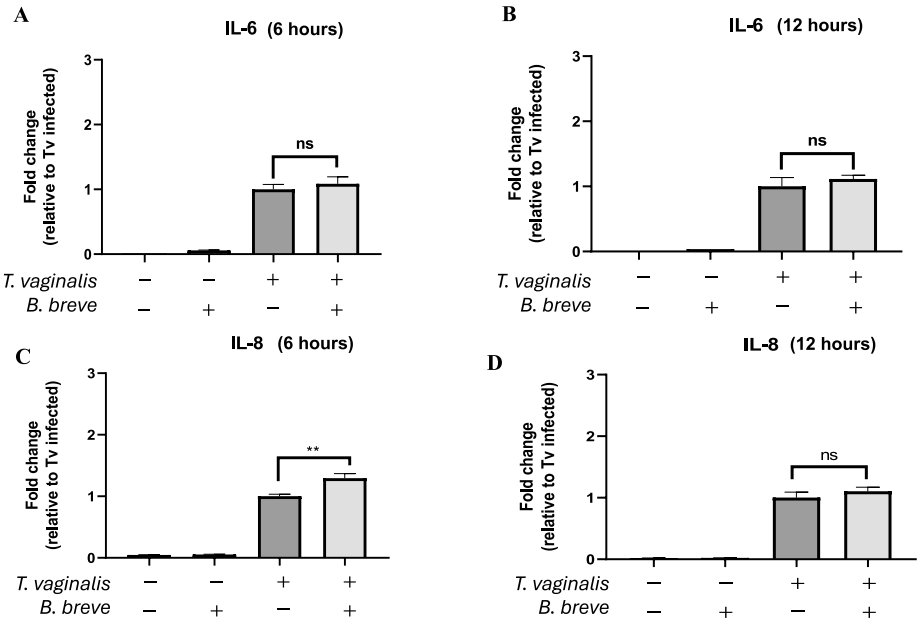

Fig. 4. Pre-colonization with *B. breve* does not alter IL-6 or IL-8 secretion in HeLa cells treated with *T. vaginalis*. HeLa cells were pretreated with viable *B. breve* followed by *T. vaginalis* infection. The IL-6 (**A and B**) and IL-8 (**C and D**) concentrations were measured by ELISA at 6 and 12 hours, respectively. $^{*}p < 0.05$; $^{**}p < 0.01$; $^{***}p < 0.001$; $^{****}p < 0.0001$; ns, not significant.

infected with *T. vaginalis* pretreated following *B. breve* pretreatment, suggesting a short-term stimulatory effect. In addition, IL-6 levels increased in the heat-killed *B. breve* group (**Supplementary Fig. S1**), likely reflecting immune activation by bacterial structural components.

In summary, these findings suggest that *B. breve* does not confer cytoprotective or anti-inflammatory benefits during *T. vaginalis* infections. Instead, early exposure to *B. breve* may transiently enhance pro-inflammatory cytokine responses in host epithelial cells.

Simultaneous exposure to *B. breve* and *T. vaginalis* does not alter HeLa cellular responses.

To determine whether *B. breve* competes with *T. vaginalis* for attachment to epithelial cells and thereby affects parasite cytoadherence and the subsequent epithelial damage, HeLa cells were co-treated with both organisms simultaneously and monitored for 6 and 12 hours. Quantification of projected cell area showed no significant difference between the co-treatment group and the *T. vaginalis*-only group, indicating that *B. breve* did not alter the extent of *T. vaginalis*-induced cytopathic effects (Fig. 5A–B). Comparable results were observed in cells co-treated with heat-killed *B. breve* (Fig. 5C–D), further supporting the lack of competitive interference with *T. vaginalis*-mediated epithelial damage.

To evaluate potential cytoprotective effects, IL-6 and IL-8 levels were measured in the co-treated groups. At 6 hours, cells co-treated with viable *B. breve* and *T. vaginalis* exhibited higher levels of both cytokines than cells infected with *T. vaginalis* alone (Fig. 6). A similar increase was observed in the heat-killed *B. breve* co-treatment group (**Supplementary Fig. S2**), suggesting that *B. breve*—whether viable or inactivated—may transiently provoke early inflammatory responses during co-exposure.

Taken together, these findings indicate that the presence of *B. breve* does not mitigate epithelial disruption caused by *T. vaginalis*. Instead, simultaneous exposure appeared to enhance early pro-inflammatory cytokine production, highlighting the potential inflammation-promoting role of *B. breve* during the initial phase of *T. vaginalis* colonization.

Transcriptomics analysis reveals molecular regulations in *T. vaginalis* during *B. breve* treatment

Given the observed increase in viable *T. vaginalis* cells after 4 h of co-culture with *B. breve*, RNA sequencing was performed to investigate the transcriptional alterations associated with this interaction. A total of 30,648 genes were detected in the control *T. vaginalis* group and 30,748 genes in the *B. breve*–treated group (Table 1and Supplementary Table 1). Principal component analysis (PCA) showed clear separation between the two groups, demonstrating high reproducibility and confirming the suitability of the dataset for downstream analyses (Fig.

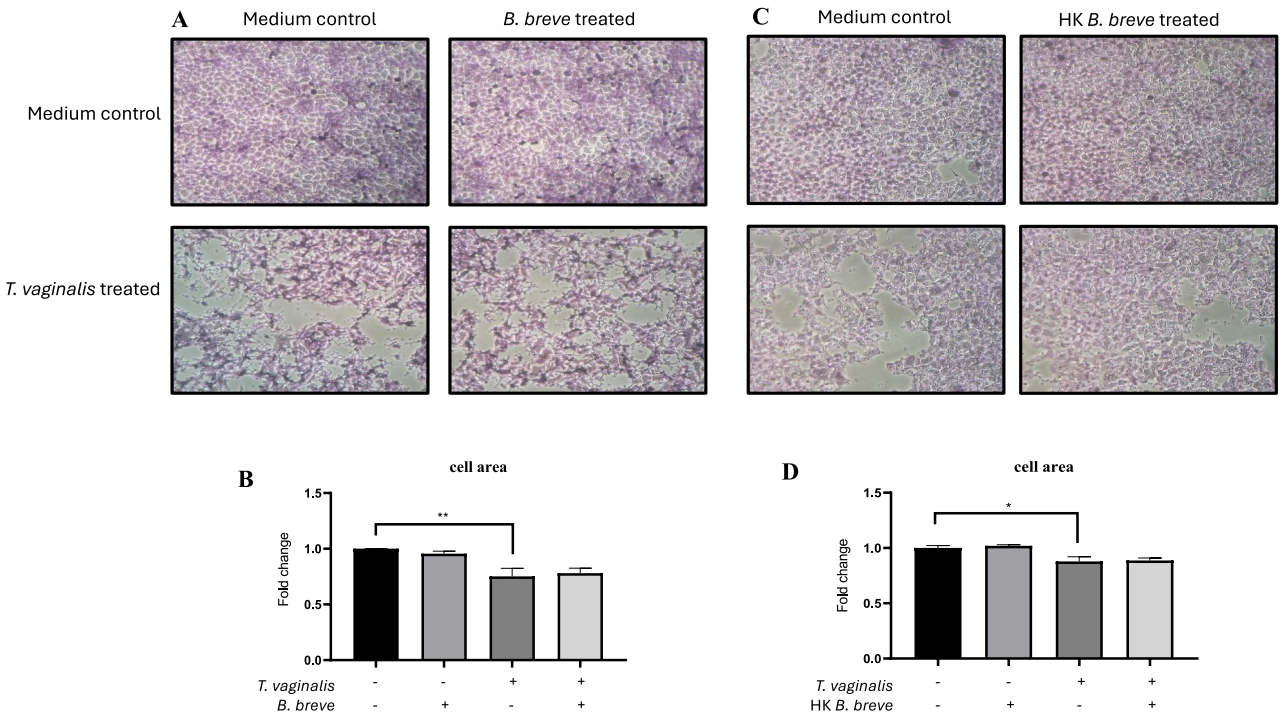

Fig. 5. Unchanged cell morphology in HeLa cells during simultaneous treatment of *B. breve* and *T. vaginalis*. The treated cells were washed, incubated, stained with Giemsa, and monitored under a microscope: (**A**) upper left, HeLa cells only; upper right, HeLa cells treated with *B. breve* for 12 hours; lower left, HeLa cells were co-cultured with *T. vaginalis* for 12 hours; lower right, HeLa was co-treated with *B. breve* and *T. vaginalis* for 12 hours. (**B**) The quantified chart of A. (**C**) The same settings as A were applied for heat-killed *B. breve* (HK-Bb) instead of viable *B. breve*. (**D**) The quantified chart of C. *p < 0.05; **p < 0.01.

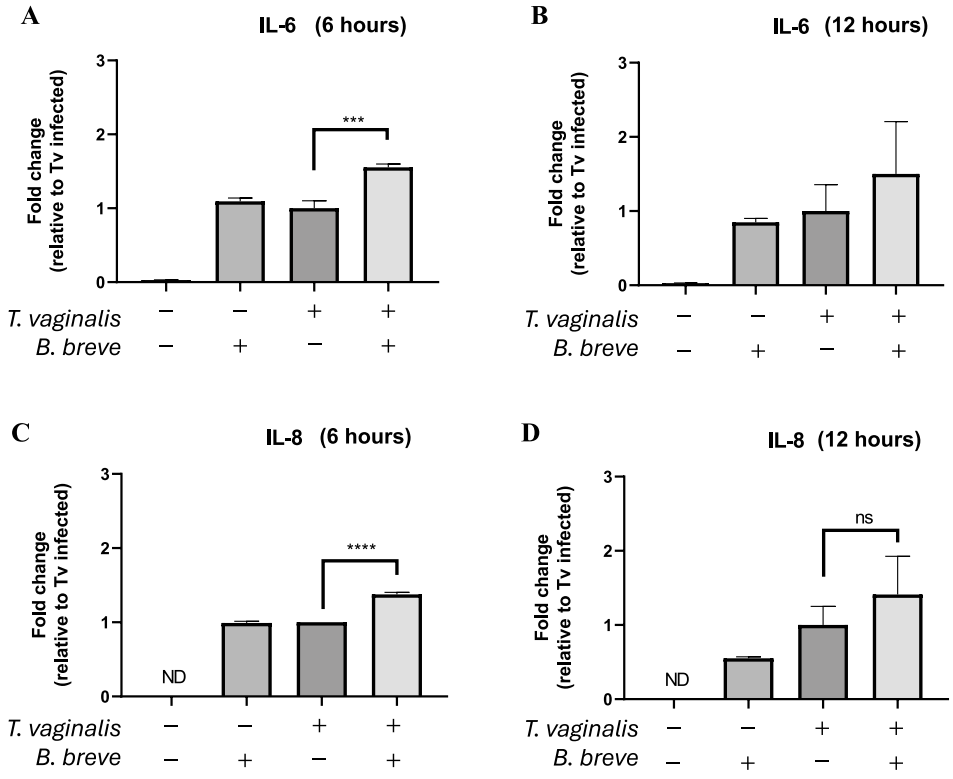

Fig. 6. Simultaneous treatment of *B. breve* and *T. vaginalis* altered IL-6 or IL-8 secretion transiently in HeLa cells. HeLa cells were co-infected with viable *B. breve* and *T. vaginalis* for tri-culture. The IL-6 (**A and B**) and IL-8 (**C and D**) concentrations were measured by ELISA at 6 and 12 hours, respectively. *p < 0.05; **p < 0.01; ***p < 0.001; ****p < 0.0001; ns, not significant.

Number of mapping genes (out of 88188)	Mapping rate (%)	
Control[a]	30648	88.77
Co-culture[b]	30748	89.39

Table 1. Statistics of transcriptomics analysis. [a]Control: *T. vaginalis* only; [b]Co-culture: *T. vaginalis* co-culture with *B. breve*. This table shows the number of genes expressed in the control and co-culture groups and the corresponding accuracy.

7A). Differential gene expression analysis identified numerous genes with significant log2 fold changes, which are presented in the heatmap in Fig. 7B.

To functionally interpret the transcriptomic data, we employed the ProFun platform[36], which integrates gene set enrichment analysis (GSEA) and Gene Ontology (GO) analyses. Upregulated genes were enriched in pathways related to DNA replication and chromatin organization, including nucleosome assembly[34,37,38], protein–DNA complex formation[39,40], and chromatin subunit organization[41,42] (Fig. 8A). These results are consistent with our earlier observation that *T. vaginalis* proliferation increased following *B. breve* exposure (Fig. 1). In addition, GO network analysis revealed significant enrichment of pathways involved in ATP synthesis–coupled electron transport (Fig. 8B), suggesting enhanced energy production.

Kyoto Encyclopedia of Genes and Genomes (KEGG) pathway analysis further demonstrated that upregulated genes were associated with energy metabolism and putative fatty acid metabolic pathways (Fig. 8C), implicating metabolic reprogramming in parasites. Supporting this interpretation, gene set variation analysis (GSVA) showed increased activity in fatty acid biosynthesis and propionate metabolism pathways (Fig. 8D). Propionate, a short-chain fatty acid (SCFA), is commonly produced by the vaginal microbiota and contributes to pH regulation and immune modulation within the vaginal environment[43–45].

Collectively, these transcriptomic and functional analyses indicated that co-culture with *B. breve* enhanced *T. vaginalis* growth by upregulating genes involved in DNA replication, energy production, and fatty acid metabolism. In particular, the activation of SCFA-related pathways, such as propionate metabolism, suggests that *B. breve* may influence *T. vaginalis* physiology via microbiota-derived metabolites.

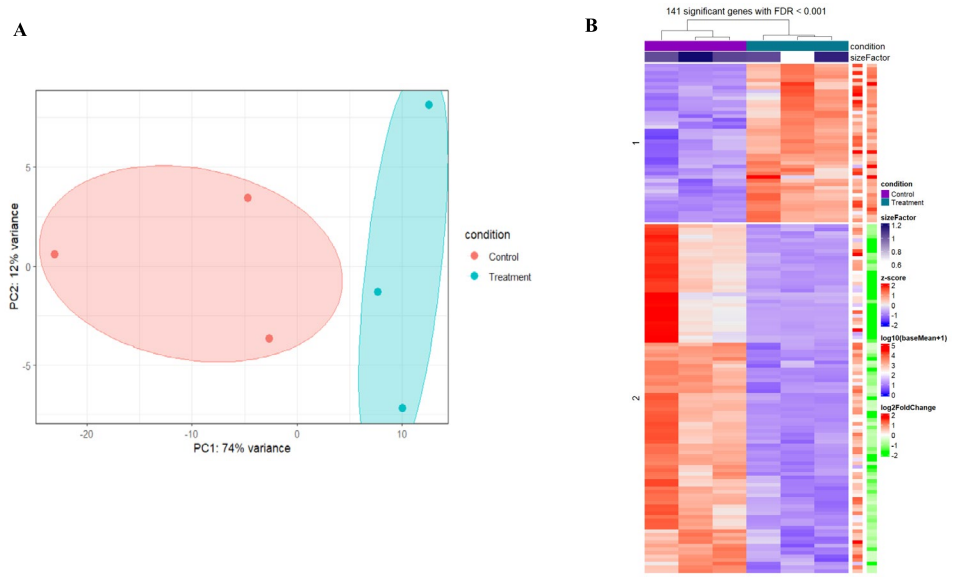

Fig. 7. PCA plot and heatmap of the comparative transcriptomics analysis. (**A**) Principal Component Analysis (PCA) was performed following Differential Expression Gene (DEG) analysis. Red dots represent the control group (triplicate), and blue dots represent the treatment group (co-culture). (**B**) The annotation bar at the top of the heatmap indicates experimental conditions. Control samples are shown in purple and treatment samples are shown in green. The upper (1) of the heatmap shows upregulated genes (red) in the control group compared to the control group, whereas the lower (2) shows downregulated genes (purple) in the co-culture group. Adjusted p-value (FDR) < 0.05.

Metabolomics analysis reinforced the impacts of *B. breve* on fatty acid metabolism in *T. vaginalis*

As noted above, transcriptomic analysis revealed significant upregulation of genes involved in fatty acid metabolism in *T. vaginalis* after co-culture with *B. breve*, whereas key genes associated with primary energy-generating pathways—including glycolysis and proteolysis/ amino acid catabolism—were not markedly altered (**Supplementary Fig. S3**). To determine whether these transcriptional changes were reflected at the metabolic level, we performed metabolomic profiling of *T. vaginalis*.

A total of 38 fatty acids containing 12 or more carbon atoms were identified and categorized into saturated fatty acids (SFAs) and unsaturated fatty acids (UFAs). After normalization to protein content, 25 metabolites were classified as UFAs and 13 as SFAs. As shown in Fig. 9, levels of several fatty acids were significantly reduced in the *B. breve*–treated group relative to the control, including 8 UFAs and 7 SFAs. This reduction suggests increased utilization of both SFA and UFA substrates, likely reflecting enhanced fatty acid metabolic activity.

These findings indicate that *T. vaginalis* undergoes metabolic adaptation in response to *B. breve*, increasing its reliance on fatty acid metabolism—possibly to support the energetic and biosynthetic demands associated with accelerated DNA replication and proliferation. This metabolic shift aligns with the observed increase in *T. vaginalis* cell numbers following co-culture.

Discussion

Probiotics are commonly used to promote vaginal health[46]; however, their interactions with protozoan pathogens, such as *T. vaginalis*, are still poorly understood. In this study, we investigated the role of *B. breve* in *T. vaginalis* infection, particularly its effect on host epithelial responses. HeLa cells were used in this research to explore the functional associations between *B. breve* and *L. gasseri*, and they also served as a commonly used epithelial model for studying *T. vaginalis*–host interactions[11,47–49]. Consistent with its known immunomodulatory properties[50,51], *B. breve* modulates the production of IL-6 and IL-8 in HeLa cells. However, when HeLa cells were pretreated with *B. breve* before *T. vaginalis* infection, cytokine production remained elevated rather than attenuated. Similarly, *B. breve* did not prevent epithelial damage or reduce *T. vaginalis* adherence, regardless of whether it was administered before or simultaneously with the parasites. These findings suggest that *B. breve* does not exert cytoprotective or anti-inflammatory effects. While *B. breve* alone elicited cytokine release, the biological relevance of this effect during *T. vaginalis* infections remains unclear. Future studies using immune cells or cytokine-conditioned media could clarify whether *B. breve*-induced signals alter immune cell behavior or influence protozoan pathogenesis.

Confocal imaging revealed a close physical association between *B. breve* and *T. vaginalis*, raising the possibility of phagocytosis. *T. vaginalis* is known to internalize yeast via actin-dependent mechanisms[27], and our transcriptomic data showed upregulation of phagocytosis-related genes (**Supplementary Fig. S4**). Similar mechanisms have been described for bacterial uptake in *Entamoeba histolytica*, and the enrichment of genes annotated to ER-mediated phagocytosis suggests a potential contribution of intracellular membranes to the

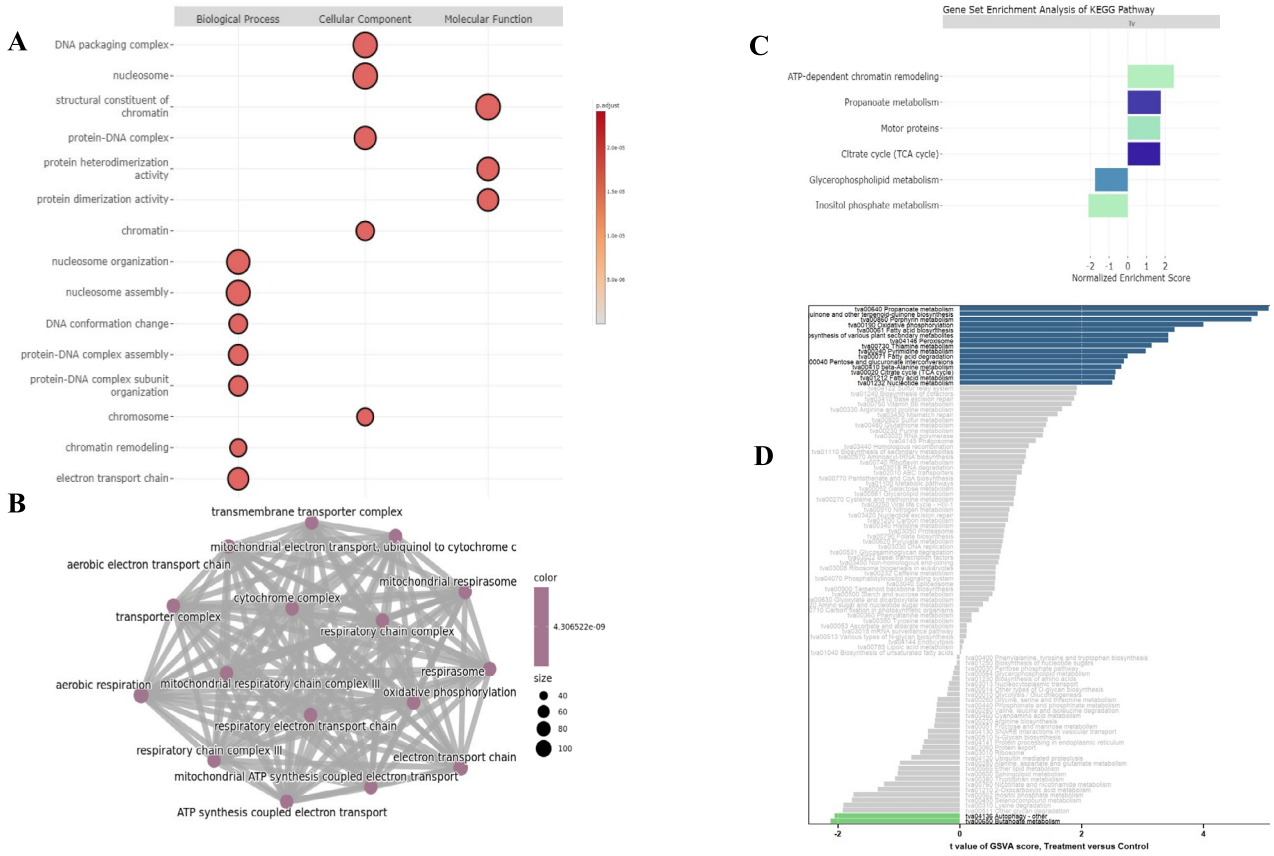

Fig. 8. Gene Ontology (GO), Gene Set Enrichment Analysis (GSEA), and Gene Set Variation Analysis (GSVA) of significantly regulated genes in *B. breve* co-cultured with *T. vaginalis*. (**A**) This GO plot showed the upregulated genes of T. vaginalis in the co-culture group. The circle size represented the gene number of the specific terms, whereas the color represented the statistical significance. (**B**) This network highlighted significant enrichment of gene sets related to the indicated biological processes. The circle size represented the gene number of the specific terms, whereas the color represented the statistical significance. (**C**) The upregulated and downregulated genes involved in biological pathways according to the Kyoto Encyclopedia of Genes and Genomes (KEGG) were shown, with different colors of bars representing the statistical significance (q-value). (**D**) GSVA represented pathways significantly upregulated in the co-culture group, which were blue, whereas downregulated pathways were green. Gray bars represented no significant differences compared to the control.

engulfment process[52]. Although no direct evidence of bacterial internalization was obtained, short-term co-culture with live-cell imaging may clarify whether *B. breve* is internalized or remains surface-bound.

Although *B. breve* is generally regarded as beneficial, its effects are context-dependent. Previous studies have focused on its intestinal role, where it functions synergistically with other probiotics to suppress pathogenic bacteria and promote microbial balance[53–56]. In contrast, its role within the vaginal niche remains unclear. In our short-interval co-culture model, *B. breve* did not protect epithelial cells from *T. vaginalis*-induced cytopathic effects, and its abundance decreased during the co-culture period. These findings differ from the behavior of protective species like *L. gasseri*, which inhibits *T. vaginalis* adhesion and preserves epithelial integrity[13,14,57]. Thus, although *B. breve* may support the growth of other beneficial species, its direct impact on *T. vaginalis* infection appears limited and, in certain contexts, may even be detrimental.

The pro-inflammatory cytokines IL-6 and IL-8 act as a 'double-edged sword' during *T. vaginalis* infection. While their transient elevation is vital for neutrophil recruitment and parasite clearance[58,59], probiotics like *Bifidobacterium* can also induce basal secretion to prime mucosal immunity and enhance barrier function[60]. In this context, the differential IL-6 responses observed between Figures 3 and 4 likely reflect differences in experimental context and timing, as sustained exposure to *T. vaginalis* following bacterial pre-incubation (24 h) may amplify epithelial inflammatory signaling, whereas short-term pre-treatment of HeLa cells with *B. breve* alone (6–12 h) is insufficient to elicit a comparable response. Conversely, *T. vaginalis* exploits hyperinflammation for iron acquisition and tissue invasion[60], thereby increasing susceptibility to secondary infections[61]. Thus, the ability of beneficial microbes to modulate these cytokine spikes is likely essential for vaginal homeostasis[62]. Nevertheless, further functional studies are required to determine whether such cytokine elevations ultimately favor host defense or serve as a parasitic survival strategy.

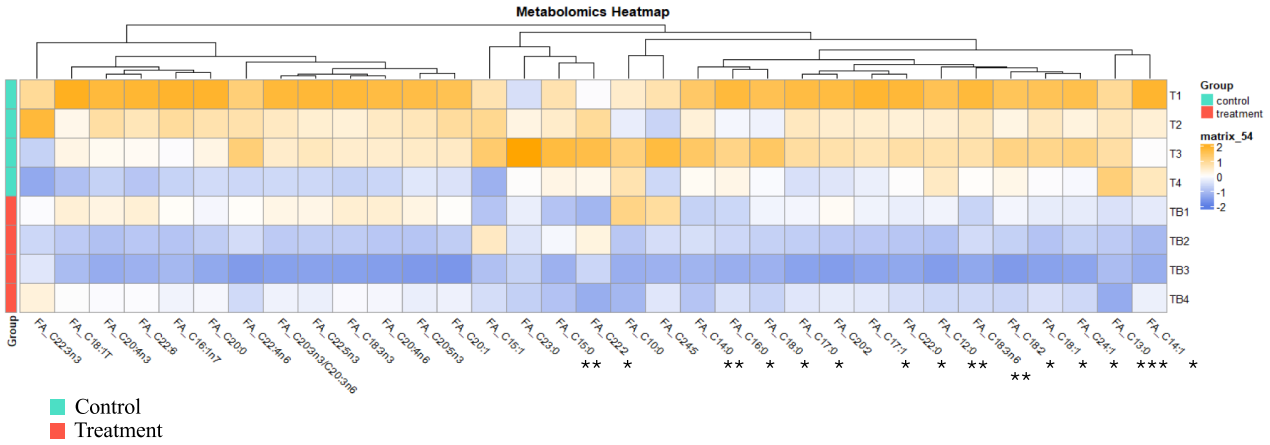

Fig. 9. The overall decrease in fatty acid concentrations in *T. vaginalis* co-cultured with *B. breve was* revealed by metabolomic analysis. Fatty acid compositions of monocultured (control, green) and co-cultured T. vaginalis with B. breve (treatment, red) for 4 hours were determined by metabolomics analysis. Four independent samples in each group were analyzed. Orange color blocks represent genes with $\log_2$ fold change > 0, while blue color blocks represent those with $\log_2$ fold change < 0. *p < 0.05; **p < 0.01.

During short-term co-incubation, *T. vaginalis* remained the dominant organism in the culture. By 24 hours, however, the interaction dynamics had shifted markedly, with *B. breve* becoming the predominant species and exhibiting substantial overgrowth—even in serum-free medium. This reversal indicates that prolonged co-culture conditions favor bacterial expansion and fundamentally alter the microbe–parasite balance, thereby limiting the interpretability of extended in vitro assays (data not shown). Consequently, analyses focused on the early time points provide a more accurate representation of the initial bacterium–protozoan interaction.

Transcriptomic analysis revealed significant upregulation of genes associated with DNA replication and fatty acid metabolism, whereas pathways related to glycolysis and amino acid catabolism were not markedly altered (**Supplementary Fig. S3**). These transcriptional findings are consistent with the observed increase in *T. vaginalis* cell numbers following *B. breve* exposure. GO and KEGG analyses further highlighted enrichment in pathways associated with ATP synthesis, nucleosome assembly, and fatty acid utilization. In addition, GSVA and GSEA indicated activation of SCFA–related pathways, particularly propionate metabolism, which is known to influence microbial growth as well as host immune regulation[43–45].

To prevent contamination of the *T. vaginalis* transcriptome by *B. breve* RNA, poly(A)-tailed mRNA was selectively captured during library preparation. Additionally, a low-speed centrifugation step was performed before harvesting the trichomonad cells to minimize the co-pelleting of bacterial cells. Consistent with these precautionary measures, the mapping rate across all transcriptomic samples remained stable (Table 1), supporting the integrity and purity of our *T. vaginalis* transcriptome dataset.

Transcriptomic analysis revealed enrichment of pathways associated with SCFA metabolism. However, SCFAs cannot be reliably quantified using conventional LC–MS without chemical derivatization due to their low molecular weights and poor ionization efficiency[49]. Therefore, to evaluate whether these transcriptional shifts corresponded to measurable metabolic changes, we performed LC-MS–based profiling of long-chain fatty acids (≥C12), which constitute the readily detectable portion of the parasite lipid pool. In total, 38 fatty acids were identified, including 25 unsaturated and 13 saturated species. Among these, 15 metabolites (8 UFAs and 7 SFAs) were significantly decreased following *B. breve* co-culture, suggesting enhanced fatty acid consumption by the parasite. These findings support the interpretation that *T. vaginalis* shifts its metabolism toward the utilization of exogenous fatty acids, potentially conserving intracellular energy for replication and contributing to increased growth. Future work will explore whether specific metabolites, such as propionate, or *B. breve*-conditioned media, can induce phenotypic changes in *T. vaginalis*. This approach aims to distinguish between contact-dependent mechanisms and effects mediated by *B. breve* secreted factors.

Notably, glycerophospholipid biosynthesis was downregulated in co-cultured *T. vaginalis*. Glycerophospholipids are central to membrane integrity, protein function, and cellular signaling[63–65], and alterations in lipid composition have been shown to influence protozoan virulence, as reported in *Leishmania* and *Plasmodium*, where lipid alterations modulate immune evasion and motility[66–68]. We therefore hypothesize that, in the presence of *B. breve*, *T. vaginalis* may reduce its own lipid synthesis to conserve biosynthetic energy and instead rely on available fatty acids to support membrane biogenesis and proliferation.

Conclusions

Our study demonstrates that *B. breve* interacts directly with *T. vaginalis*, promoting its growth and triggering transcriptional and metabolic reprogramming, particularly in fatty acid metabolism and DNA replication. Despite its known probiotic functions, *B. breve* did not confer cytoprotective or anti-inflammatory benefits to host cells challenged with *T. vaginalis*. Instead, our findings suggest that *B. breve* may help sustain microbial balance rather than acting as a direct antagonist against protozoan pathogens in the vagina. These results

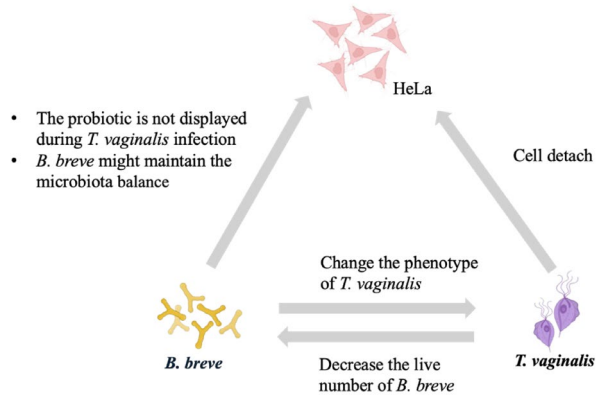

Fig. 10. The proposed role of *B. breve* during *T. vaginalis* infection. During the co-culture period, the phenotype of *T. vaginalis* was altered through direct contact with *B. breve*, while the CFU of *B. breve* was reduced. On the other hand, *B. breve* might not exert a cytoprotective role but rather help maintain microbiota balance.

highlight the complexity of host–microbe–protozoan interactions and underscore the need to further explore the context-specific roles of vaginal probiotic in infection-related ecological dynamics (Fig. 10).

Data availability

All data generated or analysed during this study are included in this published article and its supplementary information files. The datasets generated and/or analysed during the current study are available in the ArrayExpress repository under accession E-MTAB-16002.

Received: 26 November 2025; Accepted: 31 January 2026
Published online: 13 February 2026

References

1. WHO. 2018. Report on global sexually transmitted infection surveillance. World Health Organization. (2018).
2. Fichorova, R. N. Impact of T. vaginalis infection on innate immune responses and reproductive outcome. *J. Reprod. Immunol.* **83**(1–2), 185–9 (2009).
3. Primer to the Immune Response (Second Edition). Academic Cell. p. 55-83 (2014).
4. Cocomazzi, G. et al. The impact of the female genital microbiota on the outcome of assisted reproduction treatments. *Microorganisms* **11**(6), 1443 (2023).
5. Dong, W. et al. Characteristics of vaginal microbiota of women of reproductive age with infections. *Microorganisms* **12**(5), 1030 (2024).
6. De Seta, F. et al. The vaginal community state types microbiome-immune network as key factor for bacterial vaginosis and aerobic vaginitis. *Front. Microbiol.* **10**, 2451 (2019).
7. Freitas, A. C. & Hill, J. E. Quantification, isolation and characterization of Bifidobacterium from the vaginal microbiomes of reproductive aged women. *Anaerobe* **47**, 145–156 (2017).
8. Freitas, A. C. & Hill, J. E. *Bifidobacteria* isolated from vaginal and gut microbiomes are indistinguishable by comparative genomics. *PLoS One* **13**(4), e0196290 (2018).
9. Vazquez-Gutierrez, P. et al. High iron-sequestrating *Bifidobacteria* inhibit enteropathogen growth and adhesion to intestinal epithelial cells in vitro. *Front. Microbiol.* **7**, 1480 (2016).
10. Huiting Fang, H. L. et al. Bifidobacterium breve CCFM1310 enhances immunity in immunosuppressed mice via modulating immune response and gut microbiota. *Food Biosci.* **59**, 104058 (2024).
11. Plummer, E. L. et al. Lactic acid-containing products for bacterial vaginosis and their impact on the vaginal microbiota: A systematic review. *PLoS One* **16**(2), e0246953 (2021).
12. Chiu, S. F. et al. Vaginal microbiota of the sexually transmitted infections caused by Chlamydia trachomatis and Trichomonas vaginalis in women with vaginitis in taiwan. *Microorganisms* **9**(9), 1864 (2021).
13. Pradines, B., Domenichini, S. & Lievin-Le Moal, V. Adherent bacteria and parasiticidal secretion products of human cervicovaginal microbiota-associated lactobacillus gasseri confer non-identical cell protection against Trichomonas vaginalis-induced cell detachment. *Pharmaceuticals (Basel)* **15**(11), 1350 (2022).
14. Phukan, N., Brooks, A. E. S. & Simoes-Barbosa, A. A cell surface aggregation-promoting factor from Lactobacillus gasseri contributes to inhibition of Trichomonas vaginalis adhesion to human vaginal ectocervical cells. *Infect. Immun.* **86**(8), 10–1128 (2018).
15. Artuyants, A. et al. Lactobacillus gasseri and Gardnerella vaginalis produce extracellular vesicles that contribute to the function of the vaginal microbiome and modulate host-Trichomonas vaginalis interactions. *Mol. Microbiol.* **122**(3), 357–371 (2024).
16. Briaud, P. & Carroll, R. K. Extracellular vesicle biogenesis and functions in gram-positive bacteria. *Infect. Immun.* **88**(12), 10–1128 (2020).
17. Liang, L. et al. Commensal bacteria-derived extracellular vesicles suppress ulcerative colitis through regulating the macrophages polarization and remodeling the gut microbiota. *Microb. Cell Fact.* **21**(1), 88 (2022).
18. Shen, L. et al. Tight junction pore and leak pathways: A dynamic duo. *Annu. Rev. Physiol.* **73**, 283–309 (2011).
19. Schulzke, J. D. et al. Perspectives on tight junction research. *Ann. N. Y. Acad. Sci.* **1257**, 1–19 (2012).
20. Sierra, L. J. et al. Colonization of the cervicovaginal space with Gardnerella vaginalis leads to local inflammation and cervical remodeling in pregnant mice. *PLoS One* **13**(1), e0191524 (2018).

21. Mitchell, C. & Marrazzo, J. Bacterial vaginosis and the cervicovaginal immune response. *Am. J. Reprod. Immunol.* **71**(6), 555–63 (2014).
22. Anton, L. et al. Common cervicovaginal microbial supernatants alter cervical epithelial function: Mechanisms by which lactobacillus crispatus contributes to cervical health. *Front. Microbiol.* **9**, 2181 (2018).
23. Hinderfeld, A. S., Phukan, N., Bär, A. K., Roberton, A. M. & Simoes-Barbosa, A. Cooperative interactions between Trichomonas vaginalis and associated bacteria enhance paracellular permeability of the cervicovaginal epithelium by dysregulating tight junctions. *Infect. Immun.* **87**(5), e00141-19 (2019).
24. Lees, A. M. & Korn, E. D. Metabolism of unsaturated fatty acids in protozoa. *Biochemistry* **5**(5), 1475–81 (1966).
25. Ramakrishnan, S. et al. Lipid synthesis in protozoan parasites: A comparison between kinetoplastids and apicomplexans. *Prog. Lipid Res.* **52**(4), 488–512 (2013).
26. Lee, S. H., Stephens, J. L. & Englund, P. T. A fatty-acid synthesis mechanism specialized for parasitism. *Nat. Rev. Microbiol.* **5**(4), 287–97 (2007).
27. Goodman, C. D. & MCFadden, G. I. Fatty acid synthesis in protozoan parasites: Unusual pathways and novel drug targets. *Curr. Pharm.* **14**(9), 901–16 (2008).
28. Tardieux, I. et al. Lysosome recruitment and fusion are early events required for trypanosome invasion of mammalian cells. *Cell* **71**(7), 1117–30 (1992).
29. Rub, A. et al. Host-lipidome as a potential target of protozoan parasites. *Microbes Infect.* **15**(10–11), 649–60 (2013).
30. Beach, D. H., Holz Jr, G. G., Singh, B. N. & Lindmark, D. G. Fatty acid and sterol metabolism of cultured Trichomonas vaginalis and Tritrichomonas foetus. *Mol. Biochem. Parasitol.* **38**(2), 175–90 (1990).
31. Kanehisa, M. et al. KEGG: Biological systems database as a model of the real world. *Nucleic Acids Res.* **53**(D1), D672–D677 (2025).
32. Kirolos, S. A., Pilling, D. & Gomer, R. H. The extracellular sialidase NEU3 primes neutrophils. *J. Leukoc. Biol.* **112**(6), 1399–1411 (2022).
33. Meliton, A. Y. et al. Mechanical induction of group V phospholipase A(2) causes lung inflammation and acute lung injury. *Am. J. Physiol. Lung Cell. Mol. Physiol.* **304**(10), L689-700 (2013).
34. Pereira-Neves, A. & Benchimol, M. Phagocytosis by *Trichomonas vaginalis*: New insights. *Biol. Cell* **99**(2), 87–101 (2007).
35. Cardoso, F. G. & Tasca, T. Advancements in vaginal microbiota, *Trichomonas vaginalis,* and vaginal cell interactions: Insights from co-culture assays. *Microb. Cell* **15**(12), 109–118 (2025).
36. Huang, P. J. et al. *ProFun:* A web server for functional enrichment analysis of parasitic protozoan genes. *J. Microbiol. Immunol. Infect.* **57**(3), 509–517 (2024).
37. Serra-Cardona, A. & Zhang, Z. Replication-coupled nucleosome assembly in the passage of epigenetic information and cell identity. *Trends Biochem. Sci.* **43**(2), 136–148 (2018).
38. Lai, W. K. M. & Pugh, B. F. Understanding nucleosome dynamics and their links to gene expression and DNA replication. *Nat. Rev. Mol. Cell Biol.* **18**(9), 548–562 (2017).
39. Fennessy, R. T. & Owen-Hughes, T. Establishment of a promoter-based chromatin architecture on recently replicated DNA can accommodate variable inter-nucleosome spacing. *Nucleic Acids Res.* **44**(15), 7189–203 (2016).
40. Sanz-Burgos, A. P. & Gutierrez, C. Organization of thecis-acting element required for wheat dwarf geminivirus DNA replication and visualization of a Rep protein–DNA complex. *Virology* **243**(1), 119–129 (1998).
41. Baris, Y. et al. Fast and efficient DNA replication with purified human proteins. *Nature* **606**(7912), 204–210 (2022).
42. Nasheuer, H. P. et al. Replication Protein A, the main eukaryotic single-stranded DNA binding protein, a focal point in cellular DNA metabolism. *Int. J. Mol. Sci.* **25**(1), 588 (2024).
43. De Biasio, A. et al. Structure of p15(PAF)-PCNA complex and implications for clamp sliding during DNA replication and repair. *Nat. Commun.* **6**, 6439 (2015).
44. Mirzaei, R. et al. Microbiota metabolites in the female reproductive system: Focused on the short-chain fatty acids. *Heliyon* **9**(3), e14562 (2023).
45. Fernandes, T., Costa-Paiva, L. H., Pedro, A. O., Baccaro, L. F. C. & Pinto-Neto, A. M. Efficacy of vaginally applied estrogen, testosterone, or polyacrylic acid on vaginal atrophy: A randomized controlled trial. *Menopause* **23**(7), 792–8 (2016).
46. Chee, W. J. Y., Chew, S. Y. & Than, L. T. L. Vaginal microbiota and the potential of Lactobacillus derivatives in maintaining vaginal health. *Microb. Cell Fact.* **19**(1), 203 (2020).
47. Alderete, J. F. & Garza, G. E. Specific nature of Trichomonas vaginalis parasitism of host cell surfaces. *Infect. Immun.* **50**(3), 701–708 (1985).
48. Miranda-Ozuna, J. F. T. et al. Glucose-restriction increases Trichomonas vaginalis cellular damage towards HeLa cells and proteolytic activity of cysteine proteinases (CPs), such as TvCP2. *Parasitology* **146**(9), 1156–1166 (2019).
49. Mohammadi Esfanjani, S. et al. Induction of TLR5, IRAK1, and NF-kappaB expression by Trichomonas vaginalis in cervical cancer cell (HeLa) and normal human vaginal epithelial cell (HVECs) lines. *J. Infect. Dev. Ctries* **17**(8), 1160–1167 (2023).
50. Anwar, M. et al. Effects of Taro (Colocasia esculenta) water-soluble non-starch polysaccharide, Lactobacillus acidophilus, Bifidobacterium breve, Bifidobacterium infantis, and their synbiotic mixtures on pro-inflammatory cytokine interleukin-8 production. *Nutrients* **14**(10), 2128 (2022).
51. Bermudez-Brito, M. et al. Cell-free culture supernatant of Bifidobacterium *breve* CNCM I-4035 decreases pro-inflammatory cytokines in human dendritic cells challenged with Salmonella typhi through TLR activation. *PLoS One* **8**(3), e59370 (2013).
52. Hanadate, Y. et al. Endoplasmic reticulum-resident Rab8A GTPase is involved in phagocytosis in the protozoan parasite Entamoeba histolytica. *Cell Microbiol.* **18**(10), 1358–73 (2016).
53. Kaewarsar, E. et al. Effects of Synbiotic Lacticaseibacillus paracasei, Bifidobacterium breve, and Prebiotics on the Growth Stimulation of Beneficial Gut Microbiota. *Foods* **12**(20), 3847 (2023).
54. Munoz-Quezada, S. et al. Competitive inhibition of three novel bacteria isolated from faeces of breast milk-fed infants against selected enteropathogens. *Br. J. Nutr.* **109**(Suppl 2), S63-9 (2013).
55. Bernet, M. F., Brassart, D., Neeser, J. R. & Servin, A. L. Adhesion of human bifidobacterial strains to cultured human intestinal epithelial cells and inhibition of enteropathogen-cell interactions. *Appl. Environ. Microbiol.* **59**(12), 4121–8 (1993).
56. Asahara, T. et al. Probiotic bifidobacteria protect mice from lethal infection with Shiga toxin-producing Escherichia coli O157:H7. *Infect. Immun.* **72**(4), 2240–7 (2004).
57. Li, Y. et al. Bifidobacterium breve-derived indole-3-lactic acid ameliorates colitis-associated tumorigenesis by directing the differentiation of immature colonic macrophages. *Theranostics* **14**(7), 2719–2735 (2024).
58. Kang, J. H. et al. Trichomonas vaginalis promotes apoptosis of human neutrophils by activating caspase-3 and reducing Mcl-1 expression. *Parasite Immunol.* **28**(9), 439–46 (2006).
59. Fichorova, R. N. et al. Trichomonas vaginalis lipophosphoglycan triggers a selective upregulation of cytokines by human female reproductive tract epithelial cells. *Infect. Immun.* **74**(10), 5773–9 (2006).
60. Riedel, C. U., Foata, F., Philippe, D., Adolfsson, O. & Eikmanns, B. J. Stephanie Blum, Anti-inflammatory effects of bifidobacteria by inhibition of LPS-induced NF-κB activation. *World J. Gastroenterol.* **12**(23), 3729–3735 (2006).
61. Shafir, S. C., Sorvillo, F. J. & Smith, L. Current issues and considerations regarding trichomoniasis and human immunodeficiency virus in African-Americans. *Clin. Microbiol. Rev.* **22**(1), 37–45 (2009).
62. Ma, B., Forney, L. J. & Ravel, J. Vaginal microbiome: Rethinking health and disease. *Annu. Rev. Microbiol.* **66**, 371–89 (2012).
63. Singer, S. J. & Nicolson, G. L. The fluid mosaic model of the structure of cell membranes. *Science* **175**(4023), 720–31 (1972).

64. Lamari, F., Rossignol, F. & Mitchell, G. A. Glycerophospholipids: Roles in cell trafficking and associated inborn errors. *J. Inherit. Metab. Dis.* **48**(2), e70019 (2025).
65. Mishra, N. N., Prasad, T., Sharma, N. & Gupta, D. K. Membrane fluidity and lipid composition of fluconazole resistant and susceptible strains of Candida albicans isolated from diabetic patients. *Braz. J. Microbiol.* **39**(2), 219–25 (2008).
66. van Zandbergen, G., Solbach, W. & Laskay, T. Apoptosis driven infection. *Autoimmunity* **40**(4), 349–52 (2007).
67. Wanderley, J. L. et al. Apoptotic mimicry: An altruistic behavior in host/Leishmania interplay. *Braz. J. Med. Biol. Res.* **38**(6), 807–12 (2005).
68. Brochet, M. et al. Phosphoinositide metabolism links cGMP-dependent protein kinase G to essential Ca^{2+} signals at key decision points in the life cycle of malaria parasites. *PLoS Biol.* **12**(3), e1001806 (2014).

Author contributions
WHC designed the experiments; CCL, PJH, and YMY performed the bioinformatics work; WHC, RL, and FMK performed the experiments; WHC wrote the manuscript; MLC, CHC, and PT revised the manuscript. All authors read and approved the final manuscript.

Funding
This work was supported by the National Science and Technology Council, Taiwan (NSTC 114-2221-E-182-044 to PJH, NSTC 111-2320-B-182A-013-MY2 to YMY, and NSTC 113-2320-B-006-033 to WHC) and Chang Gung Memorial Hospital Linkou (CMRPG3N0891-2 and CMRPG3N0201) to YMY.

Declarations

Competing interests
The authors declare no competing interests.

Additional information
Supplementary Information The online version contains supplementary material available at https://doi.org/10.1038/s41598-026-38866-0.

Correspondence and requests for materials should be addressed to P.-J.H. or W.-H.C.